The Total Error Limited by Modifying the Parameters of Zernike Moments Computation in Duplicated Images

Thuong Le-Tien and Tan Huynh-Ngoc
Department of Electrical Electronics Engineering, HCM City University of Technology, HCMUT, Ho Chi Minh City, Vietnam
Email: thuongle@hcmut.edu.vn

Tu Huynh-Kha
School of Electrical Electronics Engineering, HCM City International University, HCMIU, Ho Chi Minh City, Vietnam
Email: hktu@hcmiu.edu.vn

***Abstract*—In the paper, an effective method for reducing Geometrical Error (G.E) and Numerical Error (N.E) of Zernike moments is proposed. By running MATLAB for the proposed Zernike's algorithm, the results of our proposed methods have shown a remarkable improvement to the total error of the analysis. The new proposed technique in reducing significantly Geometrical Error is performed better than that in the traditional technique. Considering two sides of G.E, N.E minimization and the reconstructed images having their size are almost with unchanged forms compared to the original images, then the proposed method has proven its potential capability in significantly reducing the two main errors of Zernike moments computation. Finally, the copy-move-rotate detection program has written by C++ under supporting OpenCV and Boost libraries that helps to verify the authentication of images.**

***Index Terms*—tampered image detection, Zernike polynomial, geometric moments, region of interest**

I. Introduction

Many proposed algorithms have been developed for tampered image detection process such as Pixel-based, Cloning, Resampling, Color Filter Array [1], Hu moments (1962), Fourier–Mellin moments and radial moments (Sheng and Duvernoy, 1986) [2], KPCA, PCA, etc. However, Zernike moments have proved its superiority in the analysis of invariant points of a digital image. Moreover, in the cutting process of a tampered image by Zernike moments, it also causes two main errors [2], [3]. The study on reducing G.E and N.E in the paper will help our computation to be accurate and its detection performing to achieve more highly efficient.

In a color image, there are some invariant points on their phase and magnitude within each specific small area belonged to an image. When it is copied and moved from this area to other one, the invariant points of the copied area are not changed when they located in another area.

Manuscript received September 15, 2014; revised December 21, 2014.

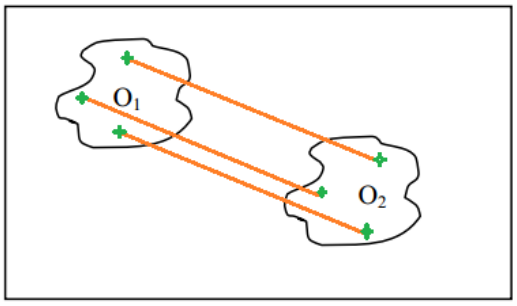

Figure 1. Forgery model (O_1 original area; O_2 copied area of O_1 area)

Therefore, using Zernike moments, it is able to detect easily the copied areas of a tampered image (Fig. 1).

To compute the Zernike moments for tampered image, a discrete-space image $f(x, y)$, which is combined by its (NxN) sub-images or Region of Interest (ROI), is mapped to the unit disc in polar form. Pixels fall outside the disc are not computed. Then, there is a moment invariance of the Zernike moment magnitude as reflected in the image mapping to the disc.

The unit circle (disc) is the assemblage of Zernike polynomials, which are orthogonal, identified in form of the polar coordinates. Considering the orthogonal Zernike polynomials of order n repetition m is

$$V_{nm}(x,y) = V_{nm}(r,\theta) = R_{nm}(r)\exp(jm\theta) = \begin{cases} N_{nm}R_{nm}(r)\cos(m\theta), \ for \ m \geq 0 \\ -N_{nm}R_{nm}(r)\sin(m\theta), \ for \ m < 0 \end{cases} \quad (1)$$

where $n \in Z^+$; m is an integer defining the rotation subject to the conditions $n - |m|$ = even, $|m| \leq n$; r is the length of the vector from origin to pixel coordinate (x , y) ; $\theta = \angle(r, x)$ in counter clockwise direction, $N_{nm} = \sqrt{\frac{2(n+1)}{1+\delta_{m0}}}$ is the normalization factor, when f is a

doi: 10.12720/joace.3.6.526-532

complex-valued function on the unit circle, Zernike moment [1] for f of order n repetition m is

$$Z_{nm}^{(f)} = \frac{n+1}{\pi}\iint_{D^2} f(x,y)V_{nm}^{*}(x,y)dxdy \quad (2)$$

where V_{nm}^{*} is a complex conjugate of V_{nm}, $D^2 : x^2 + y^2 \le 1$. Moreover, if F is the digital image of f, the above equation as below

$$Z_{nm}^{(F)} = \frac{n+1}{\pi}\sum_x\sum_y F(x,y)[V_{nm}(x,y)]^{*} \quad (3)$$

where $x^2 + y^2 \le 1$. Eq. (3) is the discrete version of Green's theorem for computing along the image's object boundary points. The Zernike real-valued radial polynomials are given by

$$R_{nm}(r) = \sum_{s=0}^{(n-|m|)/2} (-1)^s \frac{(n-s)!}{s!\left(\frac{n+|m|}{2}-s\right)!\left(\frac{n-|m|}{2}-s\right)!} r^{n-2s} \quad (4)$$

where $n-|m|$ is even, $0 \le |m| \le n$ and $n \ge 0$. Eq. (4) implies that $R_{n,m}(r) = R_{n,-m}(r)$ and $R_{nm}(r) = 0$ when $n-|m| = 0 \pmod 2$, $|m| \le n$ not satisfied. Thus, from [4],

$$\lim_{s\to(n-k)/2} V_{nm}(x,y) = \lim_{s\to(n-k)/2} R_{nm}(r)e^{jm\theta} \quad (5)$$

$$V_{nm}(x,y) = \sum_{k=m}^{n} B_{nmk} r^k e^{jm\theta} \quad (6)$$

where $$B_{nmk} = \frac{(-1)^{\frac{n-k}{2}}\left(\frac{n+k}{2}\right)!}{\left(\frac{n-k}{2}\right)!\left(\frac{k+m}{2}\right)!\left(\frac{k-m}{2}\right)!} \quad (7)$$

And k is a dynamic variable since computing $B_{nmk} r^k e^{jm\theta}$

Thus, the equation of Zernike moments in polar is

$$Z_{nm} = \frac{n+1}{\pi}\int_{-1}^{1}\int_{-\pi}^{\pi}\sum_{k=m}^{n} B_{nmk} r^k e^{-jm\theta} f(r,\theta) r dr d\theta \quad (8)$$

where $dxdy = rdrd\theta$ and $-\pi \le \theta \le \pi$.

Since the Zernike moments' magnitude values are remaining identically, those image functions before (Z_{nm}) and after (Z_{nm}^{r}) rotation, the set of Zernike moments being rotated by α angle in an image as

$$Z_{nm}^{r} = Z_{nm}e^{-jm\alpha} \quad (9)$$

The extracted rotation invariant Zernike obtained

$$\left|Z_{nm}^{r}\right| = \left|Z_{nm}e^{-jm\alpha}\right| = \left|Z_{nm}\right| \quad (10)$$

Hence, the function of piecewise continuous over the unit disc for the reconstructed image expressed as

$$f(x,y) = \sum_{n=0}^{\infty}\sum_{m=0}^{n} \lambda_n Z_{nm} V_{nm}(x,y) \quad (11)$$

where Z_{nm} is calculated over the unit circle; $\lambda_n = (n+1)[\delta(A/\pi)]$ is the normalizing constant and δA is the ratio between the area of unit disc to the total number of pixels in ROI image, $\delta A = \pi / N^2$. Besides, the value of δA plays an important role to provide different values corresponding to different squares.

In the process of computing Zernike polynomials, the main errors can be expressed as [5]

$$E_{nm} = Z_{nm} - \tilde{Z}_{nm} = E_{nm}^{(g)} + E_{nm}^{(n)} \quad (12)$$

II. Overview Geometrical Error and Numerical Error

A. Geometrical Error

Since computing Zernike polynomials in polar coordinate (r,θ) with $|r| \le 1$, it requires a linear mapping process to map correctly image coordinates (i, j) to the unit circular domain $(r,\theta) \in R^2$. Therefore, the general form of mapping techniques for each ROI image to the unit disc obtained as [4], [6]

$$\begin{cases} x_i = c_1 i + c_2 \\ y_j = c_1 j + c_2 \end{cases} \quad (13)$$

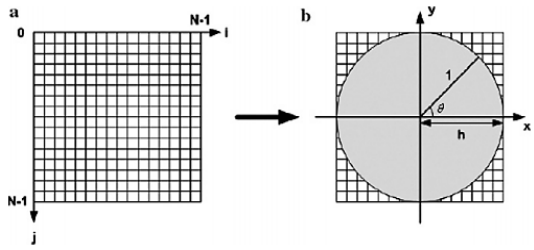

Figure 2. The $(N \times N)$ mapped to circular mapping technique

where

$$c_1 = \frac{2h}{N-1} \text{ and } c_2 = -h \quad (14)$$

In the traditional approach, the value of h is equal the radius of the unit disc ($h = 1$). Then, $c_1 = \frac{2}{N-1}$ and $c_2 = -1$. This approach causes the Geometrical Error during Zernike Moments computation.

B. Numerical Error

The numerical error $E_{nm}^{(n)}$ is created by the computation of double integral term of Zernike moments in Eq. (3) and Eq. (8). Assume that the image coordinates of a $(N \times N)$ square image and $f(x, y)$ is defined as a function of the set of point (x_i, y_j). Hence,

$$Z_{nm} = \frac{n+1}{\pi} \sum_{i=0}^{N-1} \sum_{j=0}^{N-1} f(x_i, y_j) \times \int_{x_i - \frac{\Delta x_i}{2}}^{x_i + \frac{\Delta x_i}{2}} \int_{y_j - \frac{\Delta y_j}{2}}^{y_j + \frac{\Delta y_j}{2}} V_{nm}^*(x, y) dxdy \quad (15)$$

$$, n \neq N$$

where $\Delta x_i = x_{i+1} - x_i$ and $\Delta y_j = y_{j+1} - y_j$ with $x, y \in Cartesian\ axis$. In the traditional method, the double integral term is computed by using zeroth order approximation at the center points in two intervals [6]

$$\left[x_i - \frac{\Delta x_i}{2}, x_i + \frac{\Delta x_i}{2} \right] \text{ and } \left[y_j - \frac{\Delta y_j}{2}, y_j + \frac{\Delta y_j}{2} \right].$$

The approximation for computing zeroth order is as

$$\tilde{Z}_{nm} = \frac{n+1}{\pi} \sum_{i=0}^{N-1} \sum_{j=0}^{N-1} f(x_i, y_j) V_{nm}^*(x_i, y_j) \Delta x_i \Delta y_j \quad (16)$$

$$, n \neq N$$

Hence, the total error is rewritten from (12) as

$$E_{nm} = \frac{n+1}{\pi} \sum_{i=0}^{N-1} \sum_{j=0}^{N-1} f(x_i, y_j) \times \left[\int_{x_i - \frac{\Delta x_i}{2}}^{x_i + \frac{\Delta x_i}{2}} \int_{y_j - \frac{\Delta y_j}{2}}^{y_j + \frac{\Delta y_j}{2}} V_{nm}^*(x, y) dxdy - V_{nm}^*(x_i, y_j) \Delta x_i \Delta y_j \right] \quad (17)$$

III. Proposed Method for G.E and N.E

A. Minimization of Geometrical Error

In the proposed model, the authors denoted some notations for calculating as in the Fig. 3.

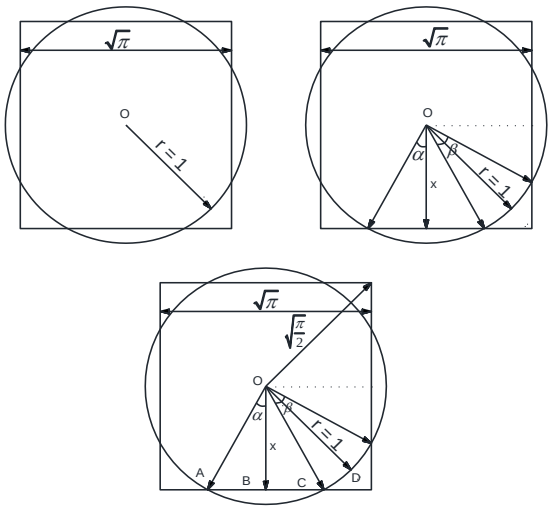

Figure 3. Analysis the squaring circle

Proved:

$r = radius\ of\ the\ circle$

$r_1 = length\ of\ a\ side\ of\ square$

$$\alpha = \cos^{-1}\left(\frac{x}{r}\right) = \cos^{-1}\left(\frac{\sqrt{\pi}}{2}\right) \rightarrow \beta = \frac{(90 - 2\alpha)\pi}{180}$$

$$\approx 0.6074753677\ (rad)$$

The area of $2\angle COD\,(or\ \beta)$ is $A_{2\angle COD} = \frac{1}{2} r^2 \beta = \frac{1}{2} \beta$.

Finally, the total numerical area inside the circle is

$$A_{total} = 4A_{2\angle COD} + 4A_{\Delta AOB} = 2\beta + 4xr \sin\alpha$$

$$\approx 2 * 0.6074753677 + 2\sqrt{\pi} \sin\left(\cos^{-1}\left(\frac{\sqrt{\pi}}{2}\right)\right)$$

$$\approx 2.857134103$$

From $A_{total} \approx 2.857134103$, the total pixels of proposed method inside unit disc are $\left\lfloor 2.857134103 \times \frac{N^2}{4} \right\rfloor$ (pixels). Hence, the efficiency (in reducing the G.E) between the proposed model (A_{remain}) and the traditional model (A'_{remain}) is computed following as

$$E = \frac{A'_{remain} - A_{remain}}{A'_{remain}} = \frac{(4r^2 - \pi r^2) - (\pi - A_{total})}{4r^2 - \pi r^2} \approx 66.862\%$$

If the size of a model image is $N \times N$ pixels, the maximum order of ZMs is n. In the Eq. 8, when denoting $\chi_{n,m,k} = \int_{-1}^{1} \int_{-\pi}^{\pi} \sum_{k=m}^{n} r^k e^{-jm\theta} f(r,\theta) r dr d\theta$, then the computational complexity of the algorithm considered below

$$\begin{cases} N^2 n \left(\frac{n}{2} + 1\right) \ multiplications \\ 2(N^2 - 1)\left(\frac{n}{2} + 1\right)^2 \ additions \end{cases}$$

Without considering $m = 0$.

In proposed method, mapping a new modified value of $h = x = \frac{\sqrt{\pi}}{2}$, $c_1 = \frac{\sqrt{\pi}}{N-1}$ and $c_2 = -\frac{\sqrt{\pi}}{2}$ is computed in Eq. (14).

Thus, $\delta A = \frac{A_{total}}{N^2} \approx \frac{2.857134103}{N^2}$.

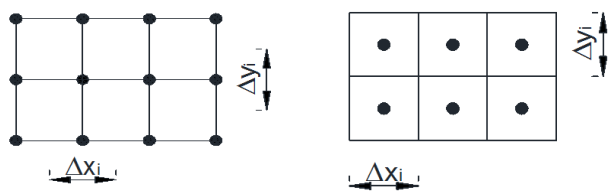

Figure 4a: Traditional approach Figure 4b: Proposed approach

B. Minimization of Numerical Error

The N.E is come about by approximating the zeroth order of the double integral term in (17). The set of Zernike moments can be computed by using the geometric moments as [7]

$$Z_{nm} = \frac{n+1}{\pi}\sum_{k=m}^{n} B_{nmk} \sum_{v=0}^{s}\sum_{u=0}^{m} w^{u} \times \binom{s}{v}\binom{m}{u} M_{k-2v-u,\,2v+u} \quad (18)$$

where $w = \begin{cases} -i\ , m > 0 \\ +i\ , m \le 0 \end{cases}$ and $s = \frac{1}{2}(k-m);\ i = \sqrt{-1}$

Otherwise, according to [1], the function of geometric moments for set of discrete points as

$$M_{nm} = \sum_{i=0}^{N-1}\sum_{j=0}^{N-1} f(x_i, y_j) H_n(x_i) H_m(y_j) \quad (19)$$

where $H_n(x_i) = \int_{x_i-\frac{\Delta x_i}{2}}^{x_i+\frac{\Delta x_i}{2}} x^n dx$; $H_m(y_j) = \int_{y_j-\frac{\Delta y_j}{2}}^{y_j+\frac{\Delta y_j}{2}} y^m dy$.

Therefore, from the Eq. (18, 19), the equation of ZMs is following as

$$Z_{nm} = \frac{2^s(n+1)}{\pi}\cdot\left(\sum_{u=0}^{m} w^u \binom{m}{u}\right)\sum_{k=m}^{n} B_{nmk} \times \sum_{v=0}^{s}\sum_{u=0}^{m}\left[\sum_{i=0}^{N-1}\sum_{j=0}^{N-1} f(x_i, y_j) H_{k-2v-u}(x_i) H_{2v+u}(y_j)\right] \quad (20)$$

Hence, (20) is a useful technique to limit the Numerical Error [1]. However, there is a tradeoff between the running time of our algorithm and the accuracy in duplicated regions detecting.

IV. Experiment Results in Matlab

In the experiment, MATLAB program (v.2011b) is used, based on the Zernike table [8], $x_i = c_1(i+0.5)+c_2$ and $y_j = c_1(j+0.5)+c_2$ with $c_1 = \sqrt{\pi}/N$, $c_2 = -\sqrt{\pi}/2$ .The results of four images are in Fig. 5 and Fig. 6.

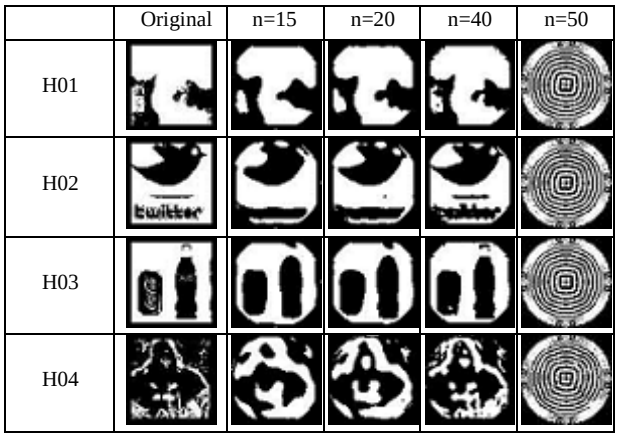

Figure 5. The reconstructed images using complex Zernike polynomials approaches with different order

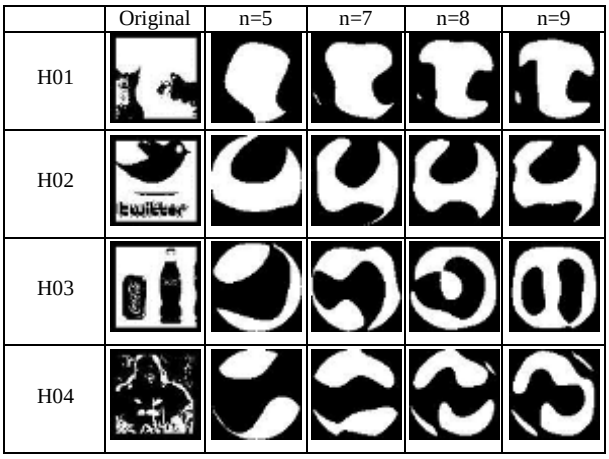

Figure 6. The reconstructed images using polar Zernike polynomials approaches with different order

The reconstruction error can be determined through [1] by the equation below

$$\varepsilon = \sum_{i=0}^{N-1}\sum_{j=0}^{N-1}\left\{\frac{\left[f(i,j)-\hat{f}(i,j)\right]^2}{\left[f(i,j)\right]^2}\right\} \quad (21)$$

where $f(i,j)$ is the continue-original image and $\hat{f}(i,j)$ is the constructed-discrete image. Thus, the difference between $f(i,j)$ and $\hat{f}(i,j)$ is the reconstruction error.

According to these above figures, the higher order n and more repetition m in Zernike computing, the more feature points extracted by ZMs. Thus, the reconstructed images are most similarly approximated to the original images. If the high orders are exceeded the capability of ZMs, the reconstructed image will be distorted. In proposed method, more feature points are highlighted that help to the detection algorithm identifying the duplicated regions having same feature points easily.

The average reconstruction error after computing between both kinds of Zernike Moments computing technique in terms of G.E and N.E are below

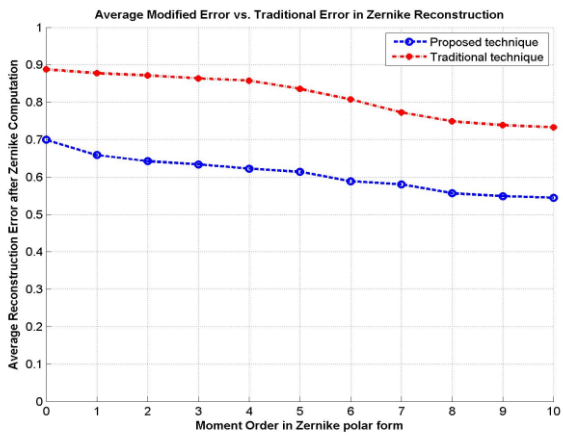

Figure 7a. The average reconstruction error between proposed technique and traditional technique of "H01" image.

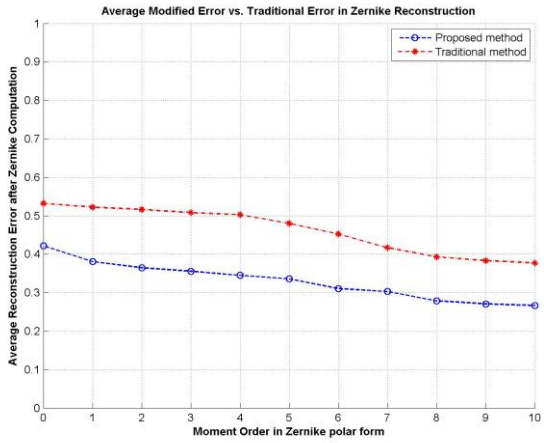

Figure 7b. The average reconstruction error between proposed technique and traditional technique of "H04" image.

The authors just shown two main graphs having the difference of total errors reduced dramatically in binary images. According to the above graphs, the G.E and N.E of proposed technique are decreased (~20.68%$|_{max}$ in Fig. 7a and ~14.35%$|_{min}$ in Fig. 7b), zeroth order to 10th order of ZMs, than that of traditional technique. Thus, the prediction for total errors is in [14.35; 20.68] (%).

V. Implementing Modified Zernike Moments to Detect a Duplicated Image

A. Overview of K-Means Clustering

The hierarchical k-means tree is combined by K-means and Hierarchical algorithm and the algorithm plays a role to split the data points at each level into K distinct region using a k-means clustering, and then applying the same method recursively to the points in each region. The recursion will be stopped when the number of points in a region is smaller than K [9], it is considered in Fig. 8.

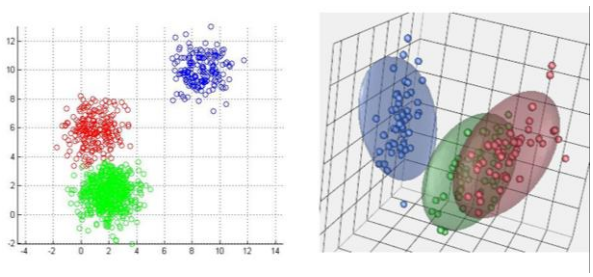

Figure 8. Hierarchical k-means clustering

Calculate Euclidean distances in each ROI image after computing ZMs and match the blocks having their similar magnitudes (Eq. 22), [10]. For comparing to other ROIs, the authors used the Bhattacharyya distances through two different classes having the variance σ_p, mean μ_p of p-th distribution, similarly for q-th have been shown below (Eq. 23).

$$d^2 = \sum_{(n,m)\in D} \sum \left(|Z_{nm}| - |Z'_{nm}|\right)^2 \quad (22)$$

$$D_B(p,q) = \frac{1}{4} ln\left(\frac{1}{4}\left(\frac{\sigma_p^2}{\sigma_q^2} + \frac{\sigma_q^2}{\sigma_p^2} + 2\right)\right) + \frac{1}{4}\left(\frac{(\mu_p - \mu_q)^2}{\sigma_p^2 + \sigma_q^2}\right) \quad (23)$$

B. Flowchart of Proposed Work

The diagram shows the steps which the authors used to extract features and detect duplicated regions in OS Linux. By studying on the tools supported OpenCV and Boost (set of color vectors processor, and vector spaces) which are able to running in Linux. The authors combined them to proposed Zernike program which has showed the successful in detecting the copied- moved regions in tampered image with the features of the program are the capability of faster detecting and scanning all areas of the photo in order to highlight feature points and find out the difference between those features. The more areas of sub-images are computed, the more feature points are detected.

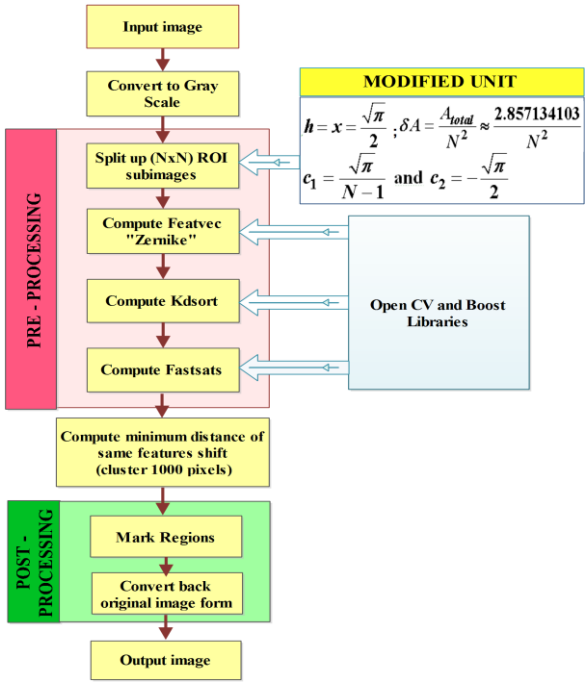

Figure 9. Flowchart of detecting a tampered image

According to Fig. 9, the color image will initially covert to gray scale, after that the Zernike algorithm will cut the image into many sub-images and then computing the set of Zernike polynomials having their modified parameters in each sub-image. With the support of OpenCV and Boost Libraries, each region having feature points will be highlighted and the through the blocks of Kdsort and Fastsats. Each feature point of sub-image will compare the value of feature point with other ones, if the distance of Euclidean and Bhattacharyya are smaller or equal than the initial threshold, the machine will mark regions coloring. Finally, the full gray image is converted back to the original color one.

The performance of ZMs compared with HU, KPCA and PCA [11] as shown in the two tables below:

$$p = \frac{T_P}{T_P + F_P}, \text{ and } r = \frac{T_P}{T_P + F_N}, F_\psi = 2.\frac{p.r}{p+r} \quad (24)$$

where T_P = the correctly detected tampered pixels; F_P = the faultily detected tampered pixels; F_N = the falsely missed pixels; p = *Precision*; r = *Recall* and F_ψ = the combination of precision and recall in a single value [12].

TABLE I. THE RESULTS (%) OF SOME METHOD TO DETECT MULTIPLE COPIES AT PIXEL LEVEL IN FIG. 10B.

Method	Precision (%)	Recall (%)	F_ψ (%)
HU	86.32	48.05	61.74
KPCA	82.51	63.20	71.57
PCA	88.01	65.47	75.08
	90.47	67.09	77.04
Average	86.83	60.95	71.36

TABLE II. THE RESULTS (%) OF SOME METHODS TO DETECT MULTIPLE COPIES AT PIXEL LEVEL IN FIG. 11B

Method	Precision (%)	Recall (%)	F_ψ (%)
HU	81.71	47.01	59.68
KPCA	84.79	61.27	71.14
PCA	86.02	63.76	73.24
ZERNIKE (proposed)	90.78	62.52	74.06
Average	85.83	58.64	69.53

It can be seen from those table, the detection algorithm of modified ZMs is better than others. The percentage of ROI image is computed inside unit disc is about 71.4% of original image and it also enhanced the number of pixels inside the unit circle. Therefore, the detection of duplicated regions is more accuracy.

Moreover, when using ZMs is not only for type *.png, but also *.jpg, the detection also shown duplicated regions well. This means the noise sensitivity of ZMs algorithm is low and it also describe well for multilevel representation in shapes of pattern. The modified method has shown its advantage for improving the capability of duplicated detection, besides that the authors could combine it with further methods to detect tampered images having additional objects from other sources.

There are some results of computing modified Zernike Moments

Figure 10a. A manipulated image of Марке Сан Лоренцо [13]

Figure 10b. The duplicated areas are detected

Figure 11a. A manipulated image of Brandenburger in Berlin [14]

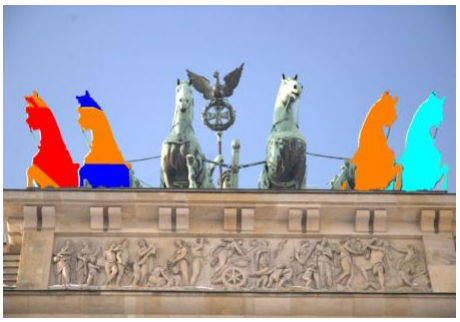

Figure 11b. The duplicated areas are detected

Figure 12a. A manipulated image of DaNang dormitory [15]

Figure 12b. The duplicated areas are detected

VI. Conclusion

In this work, the proposed method of our study is not only enhanced the number of pixels of ROI- image computed inside the unit circle but also limited the change in size of a reconstructed image after Zernike computing to compare with the size of an original image. Through the changed parameters of the size of sub-image and the support of OpenCV and Boost operating in Linux, the experiment results proved that the efficiency of detecting a tampered image by ZMs is higher than others.

References

[1] W. Chong-Yaw and R. Paramesran, "On the computational aspects of Zernike moments," *Image Vision Computing*, vol. 25, no. 6, pp. 967–980, 2007.

[2] Y. L. Sheng and L. X. Shen, "Orthogonal fourier-mellin moments for invariant pattern recognition," *Journal Optical Society America, A*, vol. 11, no. 6, pp. 1748-1757, 1994.

[3] H. Farid, "Image forgery detection-A survey," *IEEE Signal Processing Magazine*, vol. 26, no. 2, pp. 16-25, March 2009.

[4] C. W. Chong, "A formulation of a new class of continuous orthogonal moment invariants, and the analysis of their computational aspects," Ph.D thesis, Faculty of Engineering, University of Malaya, 50603 Kuala Lumpur, Malaysia, May 2003.

[5] S. X. Liao and M. Pawlak, "On the accuracy of Zernike moments for image analysis," *IEEE Trans. Pattern Anal. Mach. Intell.*, vol. 20, no. 12, pp. 1358–1364, 1998.

[6] C. W. Chong, P. Raveendran, and R. Mukundan, "A comparative analysis of algorithm for fast computation of Zernike moments," *IEEE Trans Pattern Recognition*, NY, USA, vol. 36, no. 3, pp. 731–742, 2003.

[7] C. H. The and R. T. Chin, "On image analysis by the methods of moments," *IEEE Trans. on Pattern Analysis and Machine Intelligence*, vol. 10, no. 4, pp. 496–513, 1998.

[8] [Online]. Available: http://www.lumetrics.com/documents/wavefront/Zernike_table.pdf

[9] K. Arai and A. R. Barakbah, "Hierarchical K-means: An algorithm for centroids initialization for K-means," *Reports of the Faculty of Science and Engineering*, Saga University, 840-8502 Saga Prefecture, Saga, Japan, vol. 36, no.1, pp. 25-31, 2007.

[10] S. Liao, "Image analysis by moments," Ph.D thesis, University of Manitoba, Winnipeg, Manitoba, Canada, 1993.

[11] V. Christlein, C. Riess, *et al.*, "An evaluation of popular copy-move forgery detection approaches," *IEEE Transactions on Information Forensics and Security*, vol. 7, no. 6, pp. 1841-1854, Dec 2012.

[12] I. Amerini, L. Ballan, R. Caldelli, A. D. Bimbo, and G. Serra, "A SIFT-based forensic method for copy-move attack detection and transformation recovery," *IEEE Trans. Inf. Forensics Security*, vol. 6, no. 3, pp. 1099–1110, Sep. 2011.

[13] [Online]. Available: http://www.italiadavay.ru/public/images/marche/marche_san_lorenzo.jpg.

[14] [Online]. Available: http://www.nacht-der-wissenschaften.de/2011/ansicht.php?id=%20%20%20%20%20%20%20%20101.

[15] [Online]. Available: http://www.sggp.org.vn/anninhtrattu/2014/2/340316/.

Thuong Le-Tien was born in Saigon, HoChiMinh City, Vietnam. He got the Bachelor and Master Degrees in EE-Engineering from the HoChiMinh City University of Technology, HCMUT, Vietnam in 12-1980 and 1995 in respectively. Since May-1981 he has been a teaching assistant then the lecturer in the Telecommunications Department Ho Chi Minh City University of Technology. He spent 3 years in the Federal Republic of Germany as a visiting scholar at the Ruhr University from 1989 until 1992. He received the Ph.D. in Telecommunications from the University of Tasmania, Australia, in 9-1998. He served as Deputy Department Head for many years and had been the Telecommunications Department Head from 1998 until 2002. He had also appointed for the second position as the Director of Center for Overseas Studies since 1998 up to May-2010, His areas of specialization include: Communication Systems, Digital Signal Processing and Electronic Circuits. He has published more than 120 research articles the teaching materials for university students related to Electronic Circuits 1 and 2; Digital Signal Processing & Wavelets; Antenna & Wave Propagation, Communication Systems. Prof. Le-Tien was awarded the title as National Distinguished Lecturer and various certificates for his engineering education contributions from the Academic State Council and the Chairman of National. He has been a member of the IEEE since 1996.

Huynh Ngoc Tan received the Bachelor of Engineering in Electronics-Telecommunications in November, 2014 from the Ho Chi Minh University of Technology (HCMUT), HoChiMinh City, Vietnam. In March, 2015, he will be a Master student in University of Applied Science Mannheim, Germany. Currently, he is working in Forensics group of Prof. Thuong-Le Tien at Department of Electrical-Electronics Engineering in HCMUT. His research interests include computer vision, image processing, and signal processing, biomedical image processing in particular digital image analysis by applying various existing techniques and new techniques.

Tu Huynh-Kha received the Bachelor degree and Master degree in Electronics Engineering in 2001 and 2004 from Ho Chi Minh City University of Technology (HCMUT), Vietnam. At present, she is lecturer of the International University of Ho Chi Minh City and currently working toward the PhD degree in Electronics Engineering at HCMUT. Her research interests include computer vision and image forensics.